Flow Characterization to Treat Gastrointestinal Bleeding

Ahijit Banerjee

Department of Mechanical Engineering

The University of British Columbia

August 30, 2022

1 Introduction

Gastrointestinal (GI) bleeding is a rising issue affecting about 1 in every 1000 individuals worldwide (Antunes & Copelin II, 2021). The current method of treating GI bleeding is using Proton Pump Inhibitors (PPIs) (Antunes & Copelin II, 2021; Khan & Howden, 2018), they help suppress acid secretion in the region to help the bleed repair itself naturally. However, systemic reviews of the effectiveness of PPIs have shown no significant reduction in mortality rates before surgical intervention (Leontiadis et al., 2007; van der Pol et al., 2011). Drugs in powder form seem to have a higher efficacy in coagulating bleeds in the GI region similar to what we would expect for an external wound.

One of the ways of transporting powdered drugs into the GI tract is through a catheter as it is minimally invasive. The common issues faced by transporting drugs through a catheter are blockages (Hunter & Gilbert, 2013) and partial drug delivery. Blockages can render the device useless and are currently addressed by increasing the pressure at the inlet or transporting a larger proportion of drugs than required at the wound. The wastage of drugs and the inefficiencies in the flow can be addressed by understanding the flow through a catheter.

The flow through a pipe is extensively studied, however the primary forces affecting the flow change when the diameter of the pipe is about as small as a catheter. The lubrication approximation (Papanastasiou, 1989; Tavakol, Froehlicher, Holmes, & Stone, 2017) has generally been used to simplify solving the flow through a mini pipe as its radius is much smaller than its length. However, more recent models show that the lubrication approximation fails to account for the presence of radial velocities in the flow (Venerus, 2006) which is generally not observed in a regular pipe flow.

The theoretical models presented by Venerus closely resembled the results obtained from experiments (Dutkowski, 2008) and numerical simulations (Guo & Wu, 1997). Despite Venerus addressing the gap in knowledge in the field regarding laminar flow through a mini tube, most complex models regarding flow in a mini tube still use the lubrication approximation. The most common reason for Venerus's findings not being incorporated into complex models for aerosol and granular particle transport is due to them being developed before Venerus published his paper.

Early experiments conflicted between which forces governed the behaviour of particles through mini tubes, Staffman (Goldsmith &

Mason, 1961) or Stokes (Karnis, Goldsmith, & Mason, 1963). Later models do show that both Staffman and Stokes forces play a critical role in the flow (Akhatov, Hoey, Swenson, & Schulz, 2008; Bhattacharya et al., 2013). However, all the models mentioned above assume that the effects of thermophoresis are negligible, which might not be the case (Luo & Yu, 2008).

In this paper, we strive to better understand the effect of lift forces on particles with diameters between 30 and 110 microns under steady isothermal conditions.

2 Governing Equations

The flow through a mini tube can be described using the three-dimensional Navier Stokes equations. The flow can be considered incompressible as its average velocity is expected to be within $5m/s$ to $25m/s$, which follows the precondition of the incompressibility assumption $v < 0.3Ma$. However, our primary method of solving these equations will be numerically, therefore we will be using the compressible Navier Stokes equations (Equation 1) as they have better convergence for low-speed incompressible flows (Turkel, 1987).

$$\frac{\partial \rho}{\partial t} + \frac{\partial (\rho u_i)}{\partial x_i} = 0 \tag{1a}$$

$$\frac{\partial (\rho u_i)}{\partial t} + \frac{\partial [\rho u_i u_j]}{\partial x_j} = -\frac{\partial p}{\partial x_i} + \frac{\partial \tau_{ij}}{\partial x_j} + \rho f_i \tag{1b}$$

Several forces act on a particle when it is being transported through a carrier gas, some of the primary forces affecting it are Saffman lift forces, thermophoresis, Brownian forces, diffusive forces, convective forces and gravity. In this paper, we shall be assuming the system to be isothermal, to ignore thermophoresis and Brownian forces, and the flow to be steady to ignore diffusive and convective forces. The Saffman lift forces (Saffman, 1965) are described in equation 2.

$$F = -6.46\mu a^2 (v-u) sgn\left(\frac{\partial u}{\partial y}\right) \left[\frac{\left|\frac{\partial u}{\partial y}\right|}{v}\right]^{\frac{1}{2}} \tag{2}$$

Here a denotes the radius of the particle, μ the dynamic viscosity, $\frac{\partial u}{\partial y}$ the wall-normal wall shear gradient and $(v-u)$ the instantaneous velocity difference between the fluid and the particle.

3 Methods

It is a cumbersome process to accurately characterize the flow and particle interaction through a mini tube solely through experimental methods. Thus, a combination of experiments and numerical simulations using *Ansys Fluent 2019 R1* (ANSYS Inc., 2019) was performed.

3.1 Numerical Simulation

Medical catheters to transport powder drugs into the GI region usually have an internal diameter of around $2mm$ and a length of approximately a meter. We, therefore, used the abovementioned dimensions to define the geometry used in the simulation. The mesh has 4092000 elements and is a combination of structured and unstructured elements as seen in Figure 1. Structured mesh elements are used in the outer section with a higher density near the wall to ensure higher accuracy of the flow solution when solving near the wall, on the other hand, an unstructured mesh is used in the core of the pipe to ensure the structured elements are symmetrical.

The model was verified against the published experimental results of Dutkowski (Dutkowski,

2008) shown in Figure 2. Dutkowski's experimental setup included a pipe which was 500mm long and with an internal diameter of 1.1mm. In their setup, the inlet velocity was varied while the outlet was always kept at gauge pressure. Unfortunately, their dataset was not publicly available and therefore a qualitative comparison was performed to ensure that the results from the model closely resembled the experimental results.

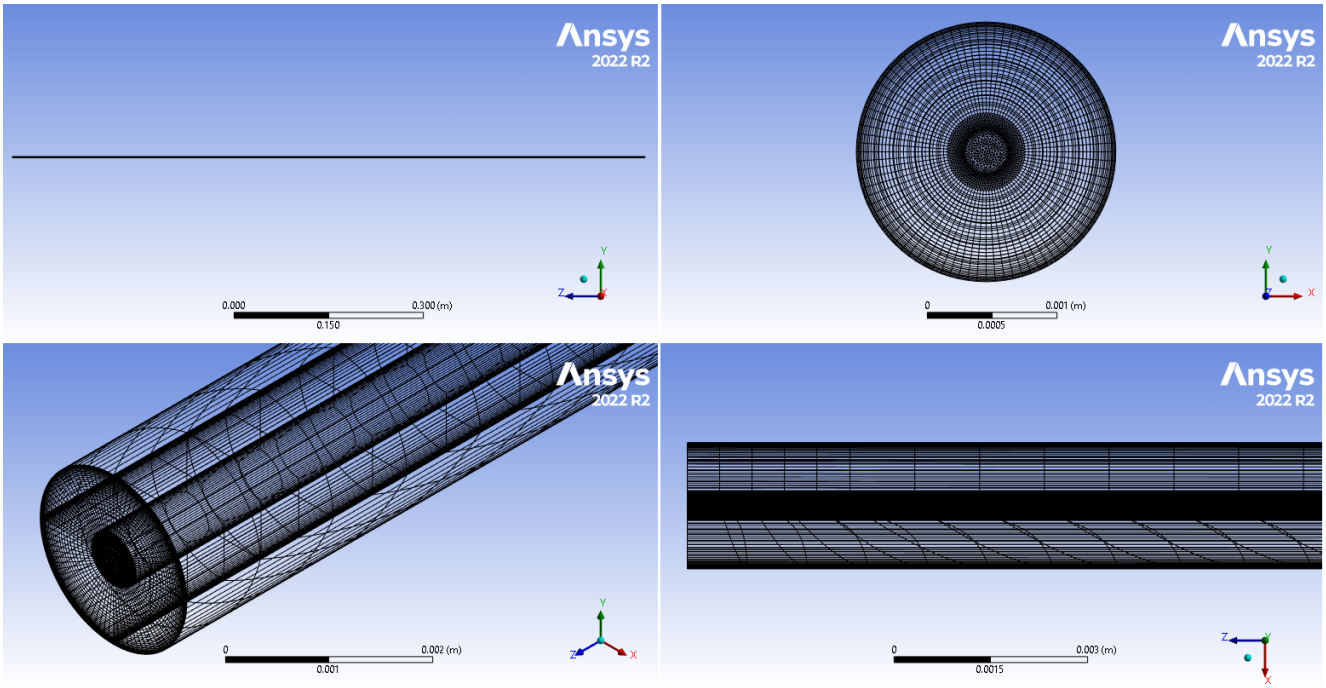

Figure 1: Geometry and Mesh for Numerical Simulation of a 400mm long pipe with an internal diameter of 2mm.

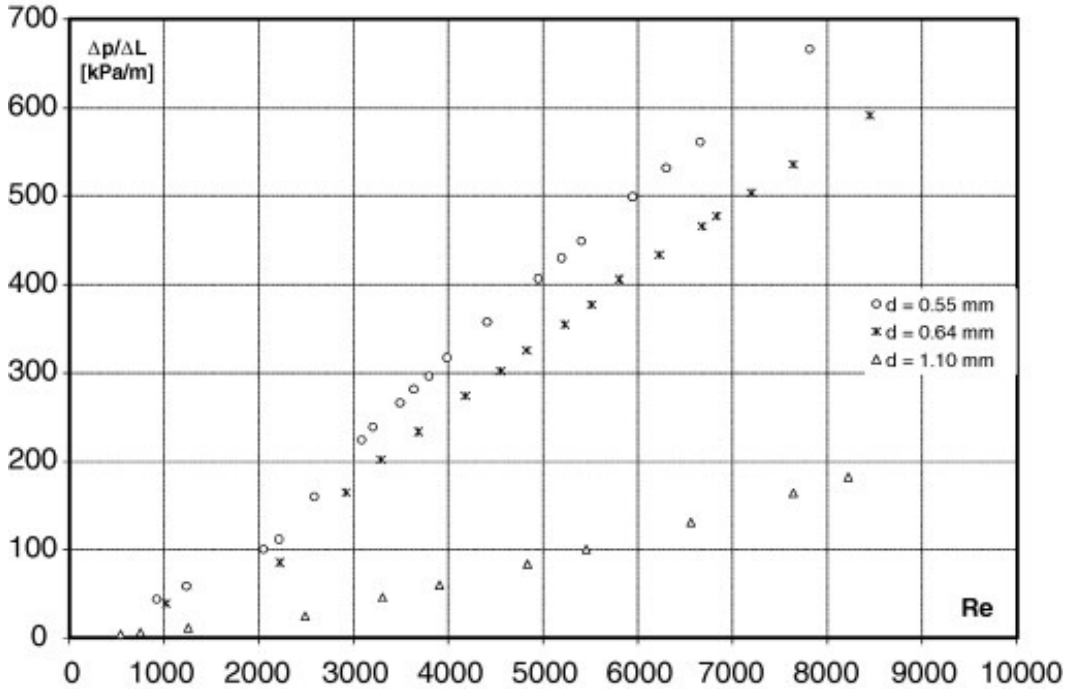

Figure 2: Experimental flow resistance of air vs. Re number in minichannels with internal diameters: 0.55, 0.64 and 1.10 mm.

The numeric simulations with the particles included in the flow were performed using a compressible solver despite the flow being incompressible due to the abovementioned reasons. The pipe has a length of $400mm$ and an internal diameter of $2mm$. The inlet velocity was kept constant at $15m/s$ and the outlet was kept at gauge pressure. Carbon dioxide was used as the working fluid instead of air as it is more representative of the actual conditions under which the device would operate. The particles used had a density of $300kg/m^3$ and were simulated using a mass flow rate of $0.001kg/s$ and an inlet velocity of $15m/s$, the same inlet velocity as the working fluid. The entire system was maintained at a constant temperature of $300K$ allowing us to investigate the effects of Saffman lift forces on changing particle size. The particle sizes varied from $10microns$ to $110microns$ and the velocity profile was measured.

3.2 Experimental Setup

The setup, shown in Figure 2, draws air from the compressed gas present in the laboratory at $115psi$ modulated by a high pressure regulator. A pressure snubber is included in-line to normalize any pressure peaks that may be present in the line. The low pressure regulator brings the pressure down to around 10–$20psi$ which acts as the inlet condition for the $610mm$ long catheter. The outlet of the catheter is connected to a pressure transducer which outputs its signal to an Arduino for post processing.

The Arduino is currently set up with a 1024 bit digital analog converter (ADS) and takes a reading from the pressure transducer every 0.1 s. The working pressure range is around 10 psi which with the ADS would give us an accurary of around 0.01 psi, but due to the limitations of the low pressure regulator we get an accuracy of around 0.5 psi.

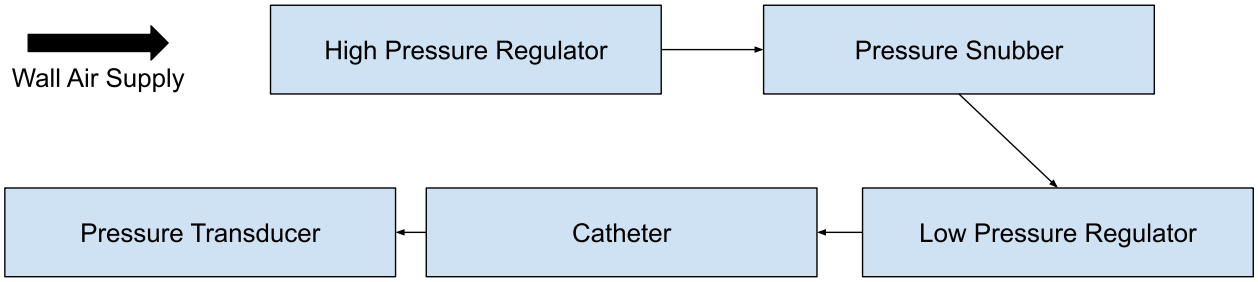

Figure 3: Experiment Setup

4 Results and Discussion

4.1 Numerical Simulation

The verification of the numerical simulation was done using both compressible and incompressible Navier-Stokes equations. For $n = 10$, we found that the compressible solver always converged while the incompressible solver never did for our simulation geometry and mesh. The observation is in line with the recommendations of Turkel (1987) of using compressible solvers for low-speed incompressible flow.

The dataset for Dutkowiski's experiment was not available, thus qualitative comparison of Figure 2 and 4 was done. On inspection, we find a very similar trend between the two plots. The experimental data appear to have a higher pressure drop per unit length than the simula-

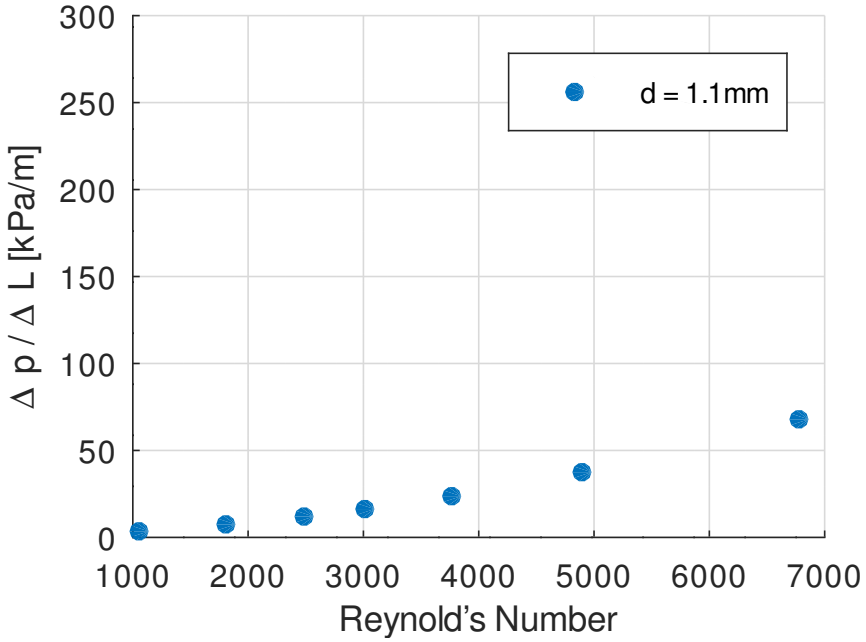

Figure 4: Numerical Results of flow resistance of air vs Re in minichannels with internal diameter of 1.10 mm.

tion, which could be due to minor friction losses in their setup that aren't calibrated for in the simulation.

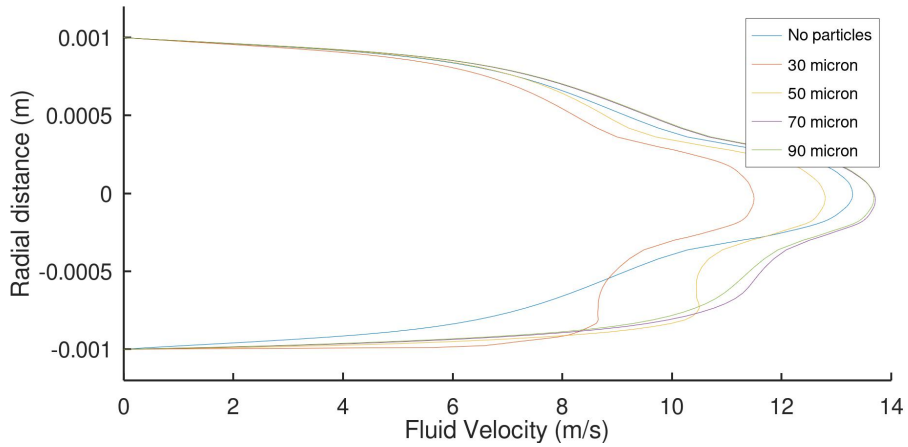

Figure 5: Velocity profile of the fluid 200mm from the inlet with varying particle diameters.

The velocity profile was analyzed for the numerical simulations with particles. In Figure 5 we observe that smaller particles distort the velocity profile to a larger extent compared to larger particles, likely due to lower inertial effects causing higher radial migration. The distortion in the bottom half of the profile is due to the effects of gravity, showing that it cannot be ignored when considering particle flow through a minitube. We also observe that the flow with larger particles has a higher peak velocity. This is likely observed because larger particles have a larger cross-sectional area for the working fluid to act on and thereby result in a higher peak velocity compared to smaller particles. On analyzing the flow along the axial direction in the

fully developed region of the flow in Figure 6, we do not observe any difference in the velocity profile due to the presence of particles.

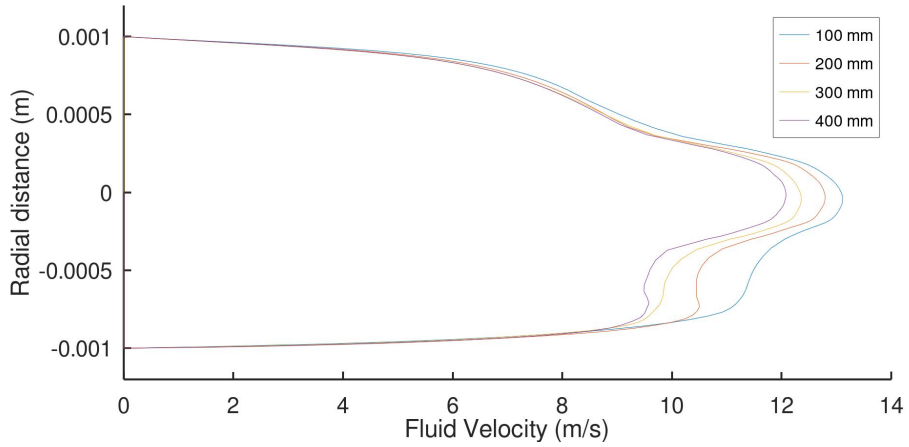

Figure 6: Velocity profile of fluid at axial distances of $100mm, 200mm, 300mm, 400mm$ from the inlet with $50micron$ particles.

4.2 Experiments

The pressure drop along the pipe was measured using the setup shown in Figure 3. A $n = 5$ measurements of pressure drop along the pipe were taken for each inlet pressure and compared against Bernoulli's equation. We observe in Figure 7 that the experimental results follow calculated results more closely for lower inlet pressures compared to higher inlet pressures. The trend might be caused by the nature of the setup where the external air source increase the pressure and velocity of the fluid simultaneously. Furthermore, since the pressure transducer blocks the outlet, the air in the entire pipe stagnates when the system stabilizes making it a complicated setup to use as a secondary verification of the numerical simulation.

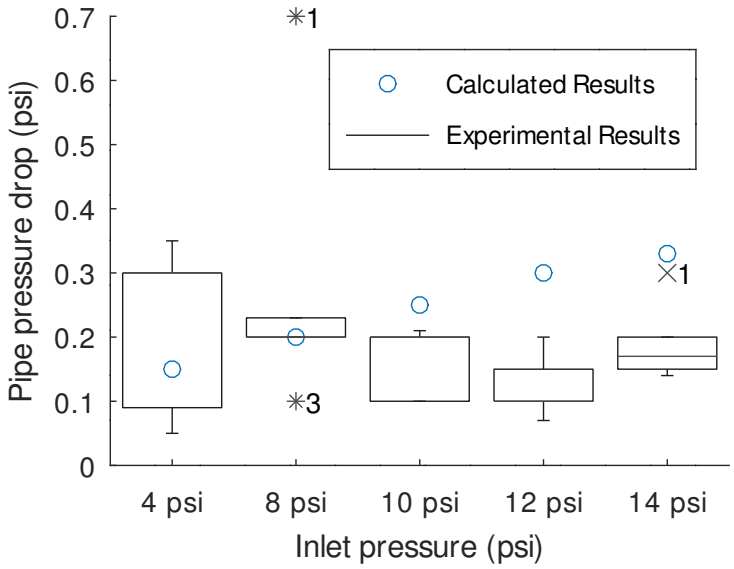

Figure 7: Pressure drop along a $610mm$ pipe with an internal diameter of $2mm$ against results from Bernoulli's equation.

5 Acknowledgments

I would like to thank the Department of Mechanical Engineering and the CREATE-U program for this opportunity. The project would not have been possible without the support and mentorship of Dr. Dana Grecov and Angelos Mavroudis. I would also like to thank Akshai Bose for his constant support and advice during the project.

References

Akhatov, I., Hoey, J., Swenson, O., & Schulz, D. (2008). Aerosol flow through a long microcapillary: collimated aerosol beam. *Microfluidics and Nanofluidics*, *5*(2), 215–224.

ANSYS Inc. (2019, Feb). *Ansys® academic research fluent r1.* Retrieved from `https://www.ansys.com/products/fluids/ansys-fluent`

Antunes, C., & Copelin II, E. L. (2021). Upper gastrointestinal bleeding. In *Statpearls [internet].* StatPearls Publishing.

Bhattacharya, S., Lutfurakhmanov, A., Hoey, J. M., Swenson, O. F., Mahmud, Z., & Akhatov, I. S. (2013). Aerosol flow through a converging-diverging micro-nozzle. *Nonlinear Engineering*, *2*(3-4), 103–112.

Dutkowski, K. (2008). Experimental investigations of poiseuille number laminar flow of water and air in minichannels. *International Journal of Heat and Mass Transfer*, *51*(25-26), 5983–5990.

Goldsmith, H., & Mason, S. (1961). Axial migration of particles in poiseuille flow. *Nature*, *190*(4781), 1095–1096.

Guo, Z., & Wu, X. (1997). Compressibility effect on the gas flow and heat transfer in a microtube. *International Journal of Heat and Mass Transfer*, *40*(13), 3251–3254.

Hunter, J. P., & Gilbert, J. A. (2013). 5 access for renal replacement therapy. *Kidney Transplantation-Principles and Practice E-Book*, 72.

Karnis, A., Goldsmith, H., & Mason, S. (1963). Axial migration of particles in poiseuille flow. *Nature*, *200*(4902), 159–160.

Khan, M. A., & Howden, C. W. (2018). The role of proton pump inhibitors in the management of upper gastrointestinal disorders. *Gastroenterology & hepatology*, *14*(3), 169.

Leontiadis, G., Sreedharan, A., Dorward, S., Barton, P., Delaney, B., Howden, C., ... others (2007). Systematic reviews of the clinical effectiveness and cost-effectiveness of proton pump inhibitors in acute upper gastrointestinal bleeding. *Health Technology Assessment (Winchester, England)*, *11*(51), iii–iv.

Luo, X., & Yu, S. (2008). Deposition of aerosol in a laminar pipe flow. *Science in China Series E: Technological Sciences*, *51*(8), 1242–1254.

Papanastasiou, T. C. (1989). Lubrication flows. *Chemical Engineering Education*, *23*(1), 50–56.

Saffman, P. G. (1965). The lift on a small sphere in a slow shear flow. *Journal of Fluid Mechanics*, *22*(2), 385–400. doi: 10.1017/S0022112065000824

Tavakol, B., Froehlicher, G., Holmes, D. P., & Stone, H. A. (2017). Extended lubrication theory: improved estimates of flow in channels with variable geometry. *Proceedings of the Royal*

Society A: Mathematical, Physical and Engineering Sciences, *473*(2206), 20170234.

Turkel, E. (1987). Preconditioned methods for solving the incompressible and low speed compressible equations. *Journal of Computational Physics*, *72*(2), 277-298. Retrieved from `https://www.sciencedirect.com/science/article/pii/0021999187900842` doi: https://doi.org/10.1016/0021-9991(87)90084-2

van der Pol, R. J., Smits, M. J., van Wijk, M. P., Omari, T. I., Tabbers, M. M., & Benninga, M. A. (2011). Efficacy of proton-pump inhibitors in children with gastroesophageal reflux disease: a systematic review. *Pediatrics*, *127*(5), 925–935.

Venerus, D. C. (2006). Laminar capillary flow of compressible viscous fluids. *Journal of Fluid Mechanics*, *555*, 59–80.